CHEMISTRY
A EUROPEAN JOURNAL

DOI: 10.1002/chem.201001816

Tunable Hydrophobicity in DNA Micelles: Design, Synthesis, and Characterization of a New Family of DNA Amphiphiles

Milena Anaya,[a] Minseok Kwak,[b] Andrew J. Musser,[b] Klaus Müllen,*[a] and Andreas Herrmann*[b]

Abstract: This work describes the synthesis and characterization of a new family of DNA amphiphiles containing modified nucleobases. The hydrophobicity was imparted by the introduction of a dodec-1-yne chain at the 5-position of the uracil base, which allowed precise and simple tuning of the hydrophobic properties through solid-phase DNA synthesis. The micelles formed from these modified DNA sequences were characterized by atomic force microscopy, dynamic light scattering, and polyacrylamide gel electrophoresis. These experiments revealed the role of the quantity and location of the hydrophobic units in determining the morphology and stability of the micelles. The effects of hybridization on the physical characteristics of the DNA micelles were also studied; these results showed potential for the sequence-specific noncovalent functionalization of the self-assembled aggregates.

Keywords: DNA hybridization · nanoparticles · nucleic acids · nucleolipids · self-assembly

Introduction

Amphiphilic molecules represent one of the fundamental building blocks of self-assembled materials. They are able to form a variety of structures of different morphology and size, depending on the hydrophobic volume and the size of the head group, as well as other variables such as concentration, temperature, pH value, and solvent. Many such structures are present in nature and play important roles in biological processes, for instance, phospholipids in the bilayers of cell membranes and intracellular vesicles. Some of these self-assembled aggregates have been reproduced in vitro and employed for potential applications such as nanoreactors,[1] gene therapy,[2] catalyst encapsulation, and drug delivery.[2a,3]

A more recent development in this field is the generation of hybrid micellar aggregates based on biopolymers, namely peptides and oligonucleotides (ODNs), covalently attached to hydrophobic moieties such as poly(propylene oxide) (PPO),[4] polystyrene,[5] linear and branched alkyl chains,[6] poly(butyl acrylate),[7] and poly(D,L-lactic-*co*-glycolic acid) (PLGA).[8] Among those hybrids, DNA-based materials are especially appealing because of the sequence programmability, self-recognition, and mechanical properties of DNA, as well as its only moderate resistance to degradation.[9] A model amphiphilic DNA-based system, the DNA block copolymer, has shown great potential for drug delivery.[10] Such micellar structures allow both facile functionalization through DNA hybridization and internalization of hydrophobic payloads.[11]

Another related class of amphiphiles is based on low-molecular-weight hydrophobic groups attached to ODNs or individual nucleotides. The latter are known as nucleolipids and have been extensively studied for their interactions with membranes, potential biomedical applications,[12] and their supramolecular organization, both into monolayers[13] and micelles.[14] The ability of these aggregates to carry information is limited by the presence of only individual nucleotides, but pyrimidine bases modified at the 5-position with a range of hydrophobic moieties have also been integrated into DNA sequences by using solid-phase synthesis.[15] The focus of these efforts, however, was not on supramolecular

[a] M. Anaya, Prof. Dr. K. Müllen
Max Planck Institute for Polymer Research
Ackermannweg 10, 55128 Mainz (Germany)
Fax: (+49) 6131-379-100
E-mail: muellen@mpip-mainz.mpg.de

[b] M. Kwak, A. J. Musser, Prof. Dr. A. Herrmann
University of Groningen, Zernike Institute for Advanced Materials
Department of Polymer Chemistry
Nijenborgh 4, 9747 AG Groningen (The Netherlands)
Fax: (+31) 50-363-4400
E-mail: a.herrmann@rug.nl

Supporting information for this article is available on the WWW under http://dx.doi.org/10.1002/chem.201001816.

aggregation but rather on the effect of the distribution of hydrophobic moieties on duplex stability.

A more common motif for this class of DNA amphiphiles is terminal functionalization at the sugar–phosphate backbone, for instance, with cholesterol[16] or long alkyl chains[17] for anchoring into lipid bilayers. Another such material containing pyrene and diacyllipid groups was recently shown to form micelles, once more with an affinity for cell membranes.[18] A final strategy utilizes solid-phase DNA synthesis with custom phosphoramidites, in which the bulky hydrophobic group completely replaces the nucleobase.[19] It is clear, then, that micellar systems of DNA amphiphiles are particularly underinvestigated, with hardly any fundamental studies on the role of the hydrophobic blocks of DNA amphiphiles, for instance, in determining the morphology of aggregates, their size and stability under dilution, or their hybridization into micelles.

In light of this, we report herein the synthesis and characterization of a family of DNA amphiphiles containing a hydrophobically modified nucleobase and an initial investigation of the influence of the positioning of these groups on micellar properties. Specifically, dodec-1-yne ($C_{12}H_{22}$) was attached to the 5-position of uracil to impart hydrophobicity, akin to reported structures.[15] The design of this precursor (**1**) allows the precise and easy introduction of hydrophobic units at arbitrary positions in a DNA sequence through conventional solid-phase synthesis. Three asymmetric lipid–DNAs were efficiently prepared through this synthetic procedure. They differed in the number and positions of the modified bases along a fixed 12-mer sequence (Scheme 1), and they all self-assembled into micelles at room temperature above a critical micelle concentration (CMC). The aggregates were studied with atomic force microscopy (AFM), dynamic light scattering (DLS), and polyacrylamide gel electrophoresis (PAGE) before and after hybridization with complementary DNA (cDNA). A strong dependence of micellar size and dilution stability on the number of hydrophobic units, as opposed to their location in the sequence, was thereby revealed.

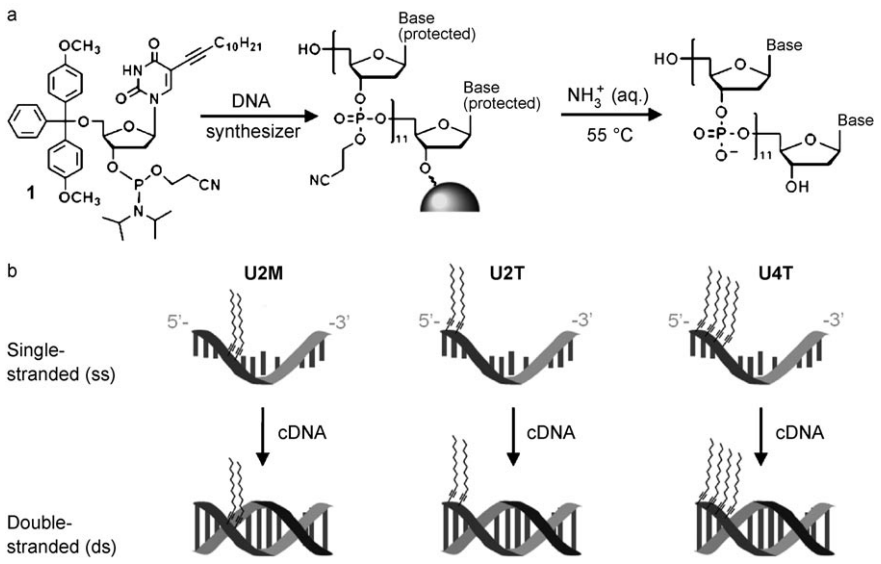

Scheme 1. Synthetic scheme and representation of lipid–DNAs. a) The precursor, 5-(dodec-1-ynyl)uracil deoxyribophosphoramidite (left) was used in conventional solid-phase DNA synthesis (center), and deprotection yielded the lipid–DNA (right). b) Schematic representation of the ss and ds lipid–DNA amphiphiles (**U2M**, **U2T**, and **U4T**) investigated.

Results and Discussion

Synthesis and micellization of lipid–DNAs: A building block analogous to deoxyuridine was synthesized, containing 5-(dodec-1-ynyl)uracil with a dimethoxytrityl (DMT) group at the 5′-position and a phosphoramidite group at the 3′-position of the deoxyribonucleoside (**1** in Scheme 1a).[20] Three different 12-mer sequences were designed: **U2M** (5′-TCCUUGGCGCAG-3′) and **U2T** (5′-UUTGGCGGATTC-3′) with two modified uracil bases and **U4T** (5′-UUUUGCGGATTC-3′) with four (U represents the modified uracil base; see Scheme 1b). Conventional solid-phase synthesis was employed by using an automated DNA synthesizer. The crude mixtures were purified by anion-exchange chromatography, with the molecular weights of the isolated products measured by MALDI-TOF mass spectrometry (see Figure S1 in the Supporting Information). Analytical HPLC results for the crude lipid–DNAs showed efficient coupling of the modified base during DNA synthesis, comparable to that attained with commercial unmodified DMT–nucleoside phosphoramidite chemicals (see Figure S2 in the Supporting Information). Furthermore, the ratio of product to byproduct in the HPLC graphs was shown to be exceptionally high. It turned out that the product band in the chromatograms showed significantly better separation from impurities than that of the natural ODNs, presumably due to the presence of the dodec-1-ynyl chains. Another effect of the modified nucleotides was found through UV/Vis spectroscopy on the lipid–DNAs (Figure 1). The **U2T** and **U4T** spectra showed broadened absorption bands and a bathochromic shift relative to a reference DNA containing unmodified dU. The degree of broadening and redshifting corresponded well to the number of modified bases in the lipid–DNAs. For further studies, the lipid–DNA solutions were heated to 95 °C and subsequently cooled to room temperature to generate micelles of uniform size.

Morphological characterization by AFM and DLS: The morphologies of all the materials in this study were characterized

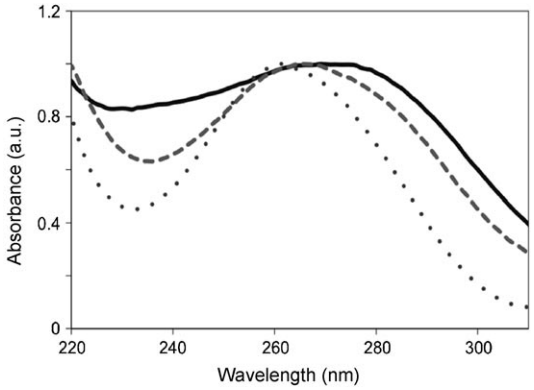

Figure 1. Normalized absorption spectra of **U4T** (——, $\lambda_{max}=269$ nm), **U2T** (-----, $\lambda_{max}=265$ nm), and DNA without modified base (•••••, $\lambda_{max}=261$ nm).

by AFM in tapping mode in fluid. This provided confirmation of micellization because well-defined round particles were observed on the mica surface in all cases (Figure 2).

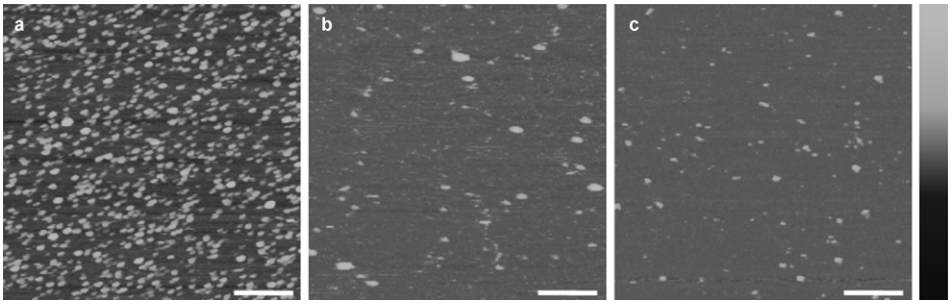

Figure 2. AFM height images of single-stranded (ss) lipid–DNA micelles: a) **U2M**, b) **U2T**, c) **U4T**. Imaging conditions were optimized for each material separately; see the Experimental Section. All scale bars are 200 nm. Vertical scale is 20 nm.

However, in spite of the close structural and chemical similarity of the three lipid–DNAs used in this study, they exhibit markedly different responses to the complicated mixture of electrostatic interactions and vertical tip forces. Indeed, a wide variation in salt and lipid–DNA concentration is observed in their optimum imaging conditions, as determined based on the coverage of well-defined micellar objects on the surface. It is already known that AFM is not an ideal tool for the quantitative characterization of soft micellar materials, because surface immobilization and compressive forces from the tip result in significantly reduced particle sizes.[21] A further complication with the materials presented herein and, presumably, with other DNA-based micelles is the observed large variation of particle size with the concentration of immobilization salt and DNA material, in some cases by nearly 50% (see Table S1 in the Supporting Information for size statistics and experimental conditions). Without a systematic investigation of the effects of salt concentration, hydrophobicity, and material concentration on observed height, rigorous micelle size data cannot be extracted from AFM studies of a family of amphiphilic materials such as that presented here. In light of these considerations, the utility of AFM in this study is restricted primarily to showing the presence of reasonably uniform micelles and highlighting the contrasts between materials. For a more reliable quantitative characterization, the much less invasive technique of DLS was employed.

The size distributions obtained from the DLS experiments yielded larger diameters than those obtained by AFM, as expected,[18,22] and are presented in Figure 3. The average hydrodynamic diameters for **U2M**, **U2T**, and **U4T** were 7.6, 7.9, and 6.7 nm, respectively. The diameter of **U4T**, containing four modified bases, is distinctly smaller (approximately 15%) than that of the lipid–DNAs with only two modifications. This observation suggests that an increase in the number of alkyl chains (of the same length) generates higher attractive hydrophobic interactions and, thereby, favors the exclusion of a greater volume of polar head groups and water from the core,[23] which is reflected as a reduction in the micelle size. On the other hand, the sizes of the micelles with sequences containing two alkyl chains, whether in the middle (**U2M**) or at the terminus (**U2T**), did not differ notably. Such a result suggests that the position of the alkyl chains in these particularly short sequences has, at most, a weak influence on morphology. This conclusion merits further investigation with a family of longer sequences with the hydrophobic bases in a range of different positions. The high-yield fully automated synthetic strategy presented herein would be well suited to such a study.

Determination of the critical micelle concentration: The CMC affords a direct measurement of the resistance of a micellar system to dissociation into unimers upon dilution, and it is commonly used to evaluate the stability of micelles.[24] Indeed, the CMC can be viewed as effectively equivalent to the free energy of micellization,[24a] with low values denoting particularly strong intermolecular interactions and favorable aggregation. The CMC of the lipid–DNAs was determined by the internalization and fluorescence of pyrene, a well-known hydrophobic probe.[8,25] The pyrene concentration was maintained at a constant level (0.6 μM), and the lipid–DNA concentrations were varied from 0.5 g L^{-1} to 0.5 mg L^{-1}.

From the fluorescence spectra of pyrene ($\lambda_{exc}=339$ nm; see Figure S6 in the Supporting Information), the change in the intensity ratio of the first and third peaks (I_1 at 373 nm and I_3 at 383 nm) was analyzed. The I_3/I_1 ratio is dependent on the polarity of the pyrene microenvironment and thus serves as a sensitive probe for the presence of micelles.[26] The I_3/I_1 value was plotted against the logarithm of the lipid–DNA concentration, and the CMC was determined

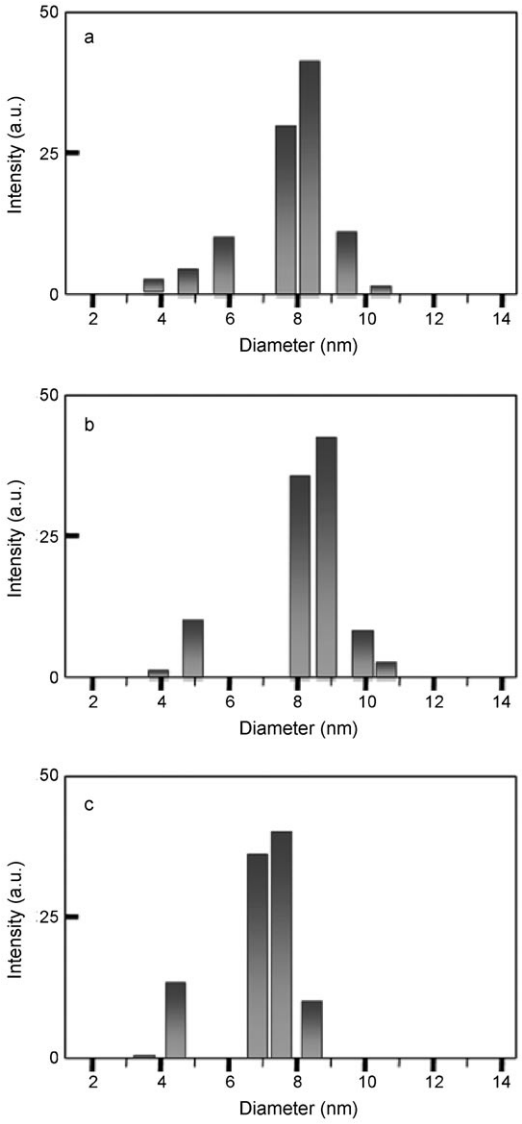

Figure 3. DLS diameter distributions, analyzed by number, of ss lipid–DNA micelles: a) **U2M**, b) **U2T**, c) **U4T**.

from the intersection of the lower horizontal asymptote of the sigmoidal curve with the tangent at the inflection point (Figure 4).

The CMC value decreased upon an increase in the number of lipid-modified bases present in the sequence, from 7.9 and 8.1 mg L^{-1} (for **U2M** and **U2T**, respectively) to 5.4 mg L^{-1} (for **U4T**). The relatively low CMC value of **U4T** shows that the micelles with four alkyl chains are thermodynamically more stable and formed more readily than those with two modifications, due to increased hydrophobic interactions. Moreover, little difference was observed between the CMC values of **U2M** and **U2T**: apparently, the proportion of hydrophobic moieties in the sequence is by far the more important determinant of micellar stability. Previously reported micelles based on DNA and diacyllipid groups,[18] PPO[4a] or PLGA[8] yielded CMCs of 0.04–0.2, 5–6, and 10 mg L^{-1}, respectively. Although the CMCs of the micelles

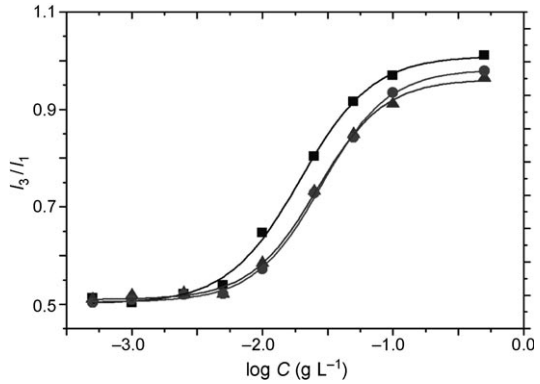

Figure 4. The change of the intensity ratios (I_3/I_1) from pyrene fluorescence ($\lambda_{exc}=339$ nm) as a function of the ss lipid–DNA concentration in water: **U2M**: ▲, **U2T**: ●, **U4T**: ■.

described in this report are higher than those of ODN/diacyllipid micelles, the values (5.4–8.1 mg L^{-1}) compare favorably with those of DNA diblock copolymer micelles.[27] More significantly, the results suggest that the CMC value can be easily tuned by modular incorporation of the appropriate number of modified nucleobases into the sequence. Further studies will be necessary, however, to probe the full range and precision of such tuning.

Hybridization with complementary DNA: The primary utility of DNA-based micellar systems is the potential for functionalization through DNA hybridization.[10a,20] For this reason, complementary DNA was hybridized onto the corona of lipid–DNA micelles to study the effects of this process on their physical characteristics, for instance, morphology and stability. Successful hybridization was confirmed by using fluorescence measurements in the presence of an asymmetric positively charged cyanine dye, SYBR green I ($\lambda_{em}=525$ nm). This dye shows exponentially greater fluorescence upon preferential binding to double-stranded (ds) DNA over ss DNA[28] with a sequence-specific response;[29] it is thus widely used for DNA staining.[30] Previous studies have reported the detection of DNA mutations by using SYBR green I, which demonstrates that the method is sufficiently sensitive to distinguish completely hybridized Watson–Crick duplexes from unstable mismatches.[28b] In light of this, SYBR green I fluorescence also allows a comparison between pristine unmodified ds DNA and ds lipid–DNAs to investigate the influence of the modified uracil bases with alkyl chains on the completeness of hybridization.

U2M, **U2T**, and **U4T** were hybridized with the respective cDNA sequences by annealing in a 1:1 molar ratio, and the products were compared with a series of control samples containing SYBR green I: ss lipid–DNA, pristine ss DNA, pristine ds DNA, and an unannealed mixture of ss lipid–DNA and its cDNA. All fluorescence spectra were collected with the same concentration of SYBR green I (1×) and DNA (15 μM) in TAE buffer (1×, 40 mM Tris-acetate, 1 mM ethylenediaminetetraacetic acid; pH 8.5). Figure 5 exhibits the results for each lipid–DNA and its controls.

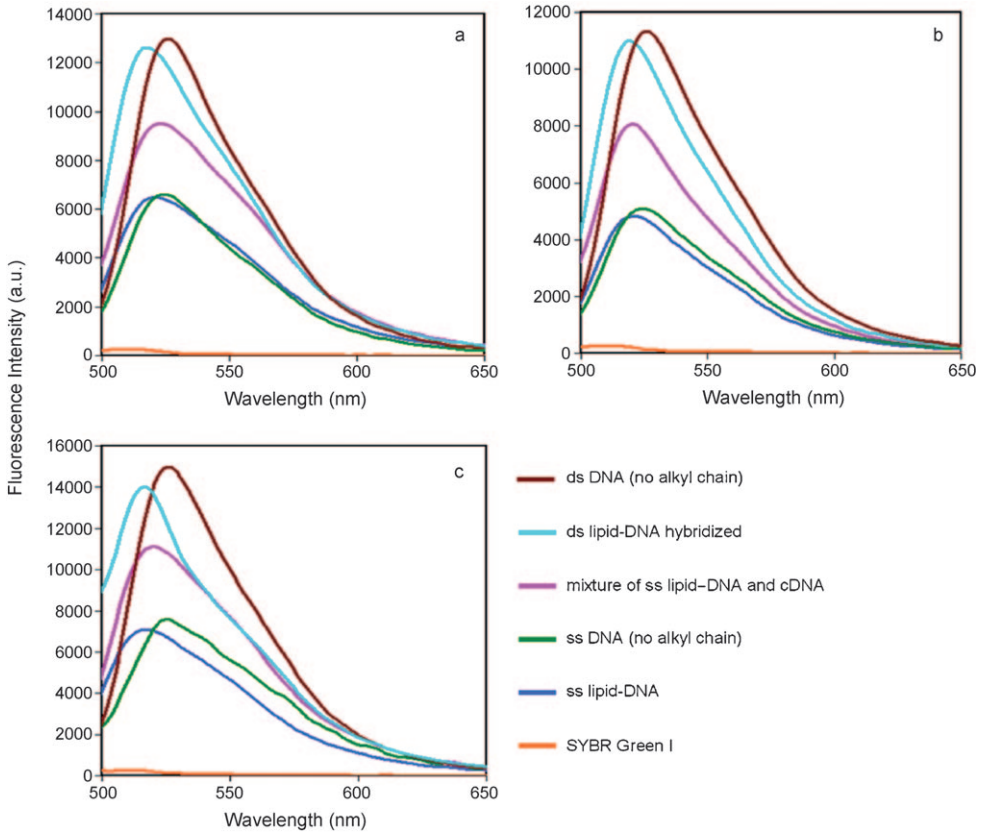

Figure 5. Fluorescence spectra of lipid–DNAs in the presence of SYBR green I and their corresponding controls: a) **U2M**, b) **U2T**, c) **U4T**. The samples, ds DNA (no lipid chain) and ds lipid–DNA hybridized, were hybridized by heating the mixture to 95 °C and subsequently cooling it to room temperature in 2 h. Other samples were measured without thermal treatment.

For all three materials, SYBR green I showed greater fluorescence intensity after hybridization, which indicates successful formation of the lipid–DNA duplexes. There is no significant intensity difference between ds lipid–DNA and ds DNA: the slight decrease in the fluorescence intensity for lipid–DNA versus pristine DNA can be attributed to molecular-weight differences. The close agreement between the peak intensities indicates that complete hybridization was accomplished along the full sequence. Additionally, there is a clear blueshift (approximately 6 nm for **U2M** and **U2T** and 10 nm for **U4T**) of the peaks of the modified DNAs relative to those of the pristine DNAs. Such a hypsochromic shift was observed in a previous study with benzimidocarbocyanine dyes containing *N*-alkyl chains, and the effect was attributed in part to the local hydrophobic environment.[31] The hydrophobicity of the modified base may play a similar role in the photophysical behavior observed here, but further investigations with a series of lipid-modified phosphoramidite precursors are required to conclusively determine the origin of this phenomenon. Nevertheless, from the SYBR green I fluorescence results, it is unambiguous that the lipid–DNAs have the full ability to hybridize.

The hybridization properties of the materials were further analyzed with 20% native PAGE (Figure 6). Under ethidium bromide staining, the gel shows discrete bands corresponding to the hybridization products of the lipid–DNAs with their respective cDNAs (Figure 6, lanes 5–7). The electrophoretic mobilities in these lanes differ significantly from those of the initial materials (Figure 6, lanes 2–4), which is

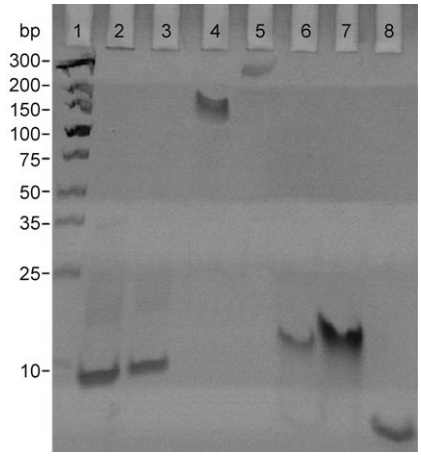

Figure 6. Native PAGE (20%) of ss and ds lipid–DNAs: Lane 1: Ultralow range ladder (10–300 bp), lane 2: **U2M**, lane 3: **U2T**, lane 4: **U4T**, lanes 5–7: hybridization products of **U4T**, **U2M**, and **U2T** with their corresponding complementary sequence (cDNA), lane 8: unmodified 12-mer DNA sequence (control).

another indication of successful duplex formation. Indeed, in none of the lanes for ds lipid–DNAs is any residual ss material visible; thus, virtually all of the material must be hybridized. Additionally, it was observed that increased incorporation of hydrophobic chains in the DNA sequences resulted in lower migration in the gel relative to the unmodified ODNs. Previous studies with spermine-modified DNA have revealed a similar behavior in PAGE experiments.[32] Howver, the mobility retardation in this case is not due to charge neutralization but rather increased molecular weight or hydrophobic interactions with the gel matrix. Furthermore, the extreme retardation of **U4T** and its hybridization product suggests that the hydrophobic interactions between these molecules are so strong that micelles are present even under the electrophoresis conditions.[18] In any case, the well-resolved bands in the gel provide clear additional confirmation of successful hybridization.

Morphological characteristics of ss and ds lipid–DNAs: After the confirmation of lipid–DNA hybridization by fluorescence spectroscopy and electrophoresis, the morphology and CMC of the ds lipid–DNAs were characterized by AFM, DLS, and pyrene solubilization. Once more, well-defined round structures were observed with AFM (Table S1 in the Supporting Information), which indicates that DNA duplex formation does not hinder micellization. It should be noted that the slight increase in the particle sizes observed in the AFM experiments for **U2T** and **U4T** (Table 1) does not necessarily reflect growth of the micelles, because the increased persistence length of ds DNA versus ss DNA[33] also results in greater resistance of the micelles to compression under the AFM tip.

Table 1. Characteristics of ss and ds lipid–DNA micelles.

Lipid–DNA	CMC [mg L^{-1}][a]		Diameter from DLS [nm]		Height from AFM [nm]	
	ss	ds	ss	ds	ss	ds
U2M	7.9	15.1	7.6±2.1	8.1±2.7	7.3±1.9	6.9±2.2
U2T	8.1	15.8	7.9±2.6	8.3±3.9	5.1±1.4	7.9±3.6
U4T	5.4	10.2	6.7±2.5	7.3±1.9	4.2±0.9	6.6±1.2

[a] Note that the higher CMC values of the ds samples are due to the molar mass of the hybridized cDNAs. The conversion into molar CMC values is presented in Table S3 in the Supporting Information.

Thus, DLS is again the preferred method to evaluate the sizes of the micelles. As shown in Table 1, all of the micelles revealed only a slight increase in diameter upon hybridization, which is consistent with reports on other DNA amphiphile micelles.[4a] This is to be expected because the close confinement of the negatively charged ss DNA strands in the corona leads to high electrostatic repulsion and consequent extension into solution. Thus, the additional rigidity imparted by hybridization does not necessarily result in significant lengthening of the DNA. The micelles of **U4T** are again somewhat smaller than those with fewer alkyl chains, which indicates that the degree of hydrophobicity remains the major factor in determining micelle size even after hybridization. Likewise, the number of hydrophobic groups still appears to be the dominant factor in the stability of the hybridized micelles, with no significant change in the molar CMC values observed after hybridization.

Conclusion

In conclusion, we have presented the synthesis of a modified nucleotide and its precise modular incorporation into short ODN sequences by using automated solid-phase DNA synthesis. The three lipid–DNA molecules characterized herein contained either two or four dodec-1-ynyluracil units at different positions in the sequence and all formed micelles at room temperature. Investigation of the micellar size and stability showed that these parameters primarily depend on the degree of hydrophobicity, with a greater number of dodec-1-ynyl chains resulting in smaller, thermodynamically more stable micelles. By contrast, the position of the hydrophobic units in the short ODNs proved to have little influence. The alkyl chains were not found to interfere with DNA hybridization, and the same trends in micelle characteristics were observed for double-stranded micelles.

The more significant outcome of this modified-base method, though, is the ability to systematically introduce well-defined hydrophobic nucleotides into DNA amphiphiles and thereby alter their supramolecular properties. This study represents the first such investigation of the fundamental role of hydrophobic moieties in determining aggregation behavior in ODN micelle systems. Further application of this strategy may eventually allow precise tuning of these structures and their physical properties. For instance, by analogy with other amphiphilic superstructures,[34] it should be possible to form self-assembled nanofibers covered with DNA and to template chemical reactions by using reactive groups introduced into the nucleobases.[35]

Experimental Section

Synthesis of the modified deoxyribouridine phosphoramidite: The modified 5-(dodec-1-ynyl)uracil-containing phosphoramidite (**1**) was synthesized in three steps as reported in a previous study by our group.[20]

DNA synthesis: The three lipid–DNAs (**U2M**, **U2T**, and **U4T**) were synthesized by employing an ÄKTA Oligopilot DNA synthesizer (GE Healthcare) on the 50 μmol scale. An ÄKTA explorer fast protein liquid chromatograhpy instrument (GE Healthcare) was used for purification and analysis of the DNA materials by employing anion-exchange chromatography with HiTrap Q HP 5 mL and 1 mL columns (GE Healthcare) under a gradient of buffer A (25 mM tris(hydroxymethyl)aminomethane–HCl (Tris-HCl); pH 8.0) and buffer B (25 mM Tris-HCl and 1.0 M NaCl; pH 8.0).

Micellization: The micelles were prepared by heating solutions (2.5 g L^{-1}) of the lipid–DNAs dissolved in ultrapure water to 95 °C and then cooling the solutions to room temperature overnight.

AFM: All AFM measurements were performed with a MultiMode 2 scanning force microscope with a Nanoscope IIIa controller (Veeco) operating in tapping mode and by using a standard fluid cell and SNL canti-

levers (f_0 = 40–75 kHz, k = 0.32 N m^{-1}; Veeco Probes, USA). Single-stranded lipid–DNA micelles were prepared for statistical height analysis as follows. A 50 μL droplet of 500 μM lipid–DNA solution in 500 μM $MgAc_2$ was deposited on freshly cleaved mica and allowed to equilibrate for 90 min. Excess solution was gently shaken off, and the sample was covered with ultrapure water (50 μL) for immediate imaging. This procedure resulted in reasonably well-formed micelles for all materials, but the concentration, salt conditions, and rinsing protocol were further optimized for each lipid–DNA separately to yield the images presented in Figure 2. For the study of single-stranded versus double-stranded lipid–DNA micelles, different conditions were employed for each lipid–DNA. For **U2M**, a 50 μL droplet of a 10 μM solution of lipid–DNA in 500 μM $MgAc_2$ was deposited on freshly cleaved mica and allowed to equilibrate for 20 min. Images were then collected. For **U2T**, a freshly cleaved mica surface was covered with 5 mM $MgAc_2$ (40 μL) and blown dry after 5 min. A 50 μL droplet of a 50 μM solution of lipid–DNA in ultrapure water was then deposited on the surface and allowed to equilibrate for 90 min. Excess solution was gently shaken off and replaced with ultrapure water (50 μL) for immediate imaging. For **U4T**, a freshly cleaved mica surface was covered with 5 mM $MgAc_2$ (40 μL) and blown dry after 5 min. A 50 μL droplet of a 1.3 μM solution of lipid–DNA in ultrapure water was then deposited on the surface and allowed to equilibrate for 20 min. Images were then collected.

DLS measurements: The size distribution of the ss and ds micelles was determined by DLS measurements at room temperature and with a scattering angle of 90° by using a ZetaSizer 3000HS instrument (Malvern Instruments Ltd., Malvern, UK) equipped with a He–Ne ion laser (633 nm). All of the solutions (2.5 g L^{-1}) were filtered through a 0.45 μm filter before the experiment and were heated up to 95 °C and cooled down to room temperature overnight. The correlation function was analyzed by the CONTIN method, and the number intensity distribution was chosen for evaluation of the data.

CMC determination: A fixed amount of pyrene was dissolved in acetone and added to several test tubes. The acetone was allowed to evaporate at 45 °C for 4 h, and DNA amphiphile solutions (concentrations ranging from 0.0005–0.5 g L^{-1}) were then added, to yield a final pyrene concentration of 0.6 μM. The solutions were incubated at 95 °C for 10 min in the dark and slowly cooled to room temperature overnight. The fluorescence spectra were recorded at room temperature by using an excitation wavelength of 339 nm. The fluorescence spectra were measured by using a Fluoroscan FL 3095 spectrometer (J&M, Germany).

DNA hybridization: The hybridization was carried out by dissolving ss lipid–DNA and the corresponding complementary sequence (molar ratio 1:1) in a solution containing TAE buffer (0.5×), NaCl (100 mM), and $MgCl_2$ (60 mM). The mixture was heated to 95 °C and then slowly cooled to room temperature (1 °C per 16 min). The hybridization was performed by a thermocycler (Biometra GmbH, Germany).

SYBR green I experiments: SYBR green I (in 1× TAE buffer, pH 8.5) was added to each DNA sample (15 μM) to give a final SYBR green I concentration of 1×. The solutions were mixed vigorously for some minutes and the fluorescence spectra were measured immediately by using a Fluoroscan FL 3095 spectrometer (J&M, Germany).

Native PAGE (20 %): Acrylamide/bisacrylamide (19:1, 40 %; 6.4 mL), 10×TBE (89 mM Tris-Base, 89 mM boric acid, 2 mM ethylenediaminetetraacetic acid; 1.3 mL), 3 % ammonium peroxodisulfate ($(NH_4)_2S_2O_8$) solution (500 μL), ultrapure water (7.4 mL), and TEMED (tetramethylethylenediamine; 15 μL) were mixed, and the solution was immediately poured between the glass plates until gel polymerization. The gel was stained with ethidium bromide and UV transillumination was at 260 nm.

Acknowledgements

This work was supported by the EU (ERC starting grant and ECCell), the Netherlands organization for scientific research (NWO-Vici), the German research foundation (DFG), and the Zernike Institute for Advanced Materials. M.K. thanks the University of Groningen (Ubbo Emmius programme), and A.J.M. thanks the Nuffic (Huygens scholarship programme).

[1] V. Kotzabasakis, E. Georgopoulou, M. Pitsikalis, N. Hadjichristidis, G. Papadogianakis, *J. Mol. Catal. A* **2005**, *231*, 93.
[2] a) J. A. Wolff, J. E. Hagstrom, S. D. Monahan, V. Budker, D. B. Rozema, P. M. Slattum, US 6.740.643 B2, **2004**; b) P. S. Kuhn, Y. Levin, M. C. Barbosa, *Phys. A* **1999**, *274*, 8.
[3] a) R. Savic, L. B. Luo, A. Eisenberg, D. Maysinger, *Science* **2003**, *300*, 615; b) Y. Kakizawa, K. Kataoka, *Adv. Drug Delivery Rev.* **2002**, *54*, 203; c) K. Kataoka, A. Harada, Y. Nagasaki, *Adv. Drug Delivery Rev.* **2001**, *47*, 113.
[4] a) F. E. Alemdaroglu, K. Ding, R. Berger, A. Herrmann, *Angew. Chem.* **2006**, *118*, 4313; *Angew. Chem. Int. Ed.* **2006**, *45*, 4206; b) K. Ding, F. E. Alemdaroglu, M. Börsch, R. Berger, A. Herrmann, *Angew. Chem.* **2007**, *119*, 1191; *Angew. Chem. Int. Ed.* **2007**, *46*, 1172.
[5] Z. Li, Y. Zhang, P. Fullhart, C. A. Mirkin, *Nano Lett.* **2004**, *4*, 1055.
[6] a) T. Gore, Y. Dori, Y. Talmon, M. Tirrell, H. Bianco-Peled, *Langmuir* **2001**, *17*, 5352; b) Y. C. Yu, P. Berndt, M. Tirrell, G. B. Fields, *J. Am. Chem. Soc.* **1996**, *118*, 12515.
[7] M. G. J. ten Cate, H. G. Börner, *Macromol. Chem. Phys.* **2007**, *208*, 1437.
[8] J. H. Jeong, T. G. Park, *Bioconjugate Chem.* **2001**, *12*, 917.
[9] J. I. Sheu, E. Y. Sheu, *AAPS PharmSciTech* **2006**, *7*, E38.
[10] a) F. E. Alemdaroglu, N. C. Alemdaroglu, P. Langguth, A. Herrmann, *Adv. Mater.* **2008**, *20*, 899; b) F. E. Alemdaroglu, N. C. Alemdaroglu, P. Langguth, A. Herrmann, *Macromol. Rapid Commun.* **2008**, *29*, 326.
[11] M. Kwak, A. J. Musser, J. Lee, A. Herrmann, *Chem. Commun.* **2010**, *46*, 4935.
[12] H. Rosemeyer, *Chem. Biodiversity* **2005**, *2*, 977.
[13] U. Rädler, C. Heiz, P. L. Luisi, R. Tampe, *Langmuir* **1998**, *14*, 6620.
[14] a) D. Berti, P. Barbaro, I. Bucci, P. Baglioni, *J. Phys. Chem. B* **1999**, *103*, 4916; b) G. Zandomeneghi, P. L. Luisi, L. Mannina, A. Segre, *Helv. Chim. Acta* **2001**, *84*, 3710; c) P. Baglioni, D. Berti, *Curr. Opin. Colloid Interface Sci.* **2003**, *8*, 55.
[15] a) L. Ötvös, J. Sági, G. Sági, A. Szemző, *Nucleosides Nucleotides* **1999**, *18*, 1929; b) F. Seela, M. Zulauf, *Helv. Chim. Acta* **1999**, *82*, 1878.
[16] I. Pfeiffer, F. Höök, *J. Am. Chem. Soc.* **2004**, *126*, 10224.
[17] Y. H. M. Chan, B. van Lengerich, S. G. Boxer, *Proc. Natl. Acad. Sci. USA* **2009**, *106*, 979.
[18] H. P. Liu, Z. Zhu, H. Z. Kang, Y. R. Wu, K. Sefan, W. H. Tan, *Chem. Eur. J.* **2010**, *16*, 3791.
[19] U. Jakobsen, A. C. Simonsen, S. Vogel, *J. Am. Chem. Soc.* **2008**, *130*, 10462.
[20] M. Kwak, I. J. Minten, D. M. Anaya, A. J. Musser, M. Brasch, R. J. M. Nolte, K. Müllen, J. J. L. M. Cornelissen, A. Herrmann, *J. Am. Chem. Soc.* **2010**, *132*, 7834.
[21] X. M. Liang, G. Z. Mao, K. Y. S. Ng, *Colloids Surf. B* **2004**, *34*, 41.
[22] C. M. Hoo, N. Starostin, P. West, M. L. Mecartney, *J. Nanopart. Res.* **2008**, *10*, 89.
[23] a) C. Tanford, *Proc. Natl. Acad. Sci. USA* **1974**, *71*, 1811; b) J. C. Leroux, A. S. Benahmed, US 6.338.859, **2002**; c) C. Tanford, *J. Phys. Chem.* **1974**, *78*, 2469.
[24] a) P. Sehgal, O. Kosaka, H. Doe, D. E. Otzen, *J. Dispersion Sci. Technol.* **2009**, *30*, 1050; b) C.-L. Lo, S.-J. Lin, H.-C. Tsai, W.-H. Chan, C.-H. Tsai, C. H. D. Cheng, G.-H. Hsiue, *Biomaterials* **2009**, *30*, 3961.
[25] a) M. Wilhelm, C. L. Zhao, Y. C. Wang, R. L. Xu, M. A. Winnik, J. L. Mura, G. Riess, M. D. Croucher, *Macromolecules* **1991**, *24*, 1033; b) G. Kwon, M. Naito, M. Yokoyama, T. Okano, Y. Sakurai, K. Kataoka, *Langmuir* **1993**, *9*, 945.
[26] K. Kalyanasundaram, J. K. Thomas, *J. Phys. Chem.* **1977**, *81*, 2176.

[27] a) Y. Y. Li, X. Z. Zhang, J. L. Zhu, H. Cheng, S. X. Cheng, R. X. Zhuo, *Nanotechnology* **2007**, *18*, 215605; b) T. Inoue, G. H. Chen, K. Nakamae, A. S. Hoffman, *J. Controlled Release* **1998**, *51*, 221.
[28] a) X. Jin, S. Yue, K. S. Wells, V. L. Singer, *Biophys. J.* **1994**, *66*, A159; b) T. Maruyama, T. Takata, H. Ichinose, L. C. Park, N. Kamaiya, M. Goto, *Biotechnol. Lett.* **2003**, *25*, 1637.
[29] R. S. Tuma, M. P. Beaudet, X. K. Jin, L. J. Jones, C. Y. Cheung, S. Yue, V. L. Singer, *Anal. Biochem.* **1999**, *268*, 278.
[30] a) J. Skeidsvoll, P. M. Ueland, *Anal. Biochem.* **1995**, *231*, 359; b) A. E. Kiltie, A. J. Ryan, *Nucleic Acids Res.* **1997**, *25*, 2945.
[31] U. D. Rossi, J. Moll, J. Kriwanek, S. Daehne, *J. Fluoresc.* **1994**, *4*, 53.
[32] a) D. A. Barawkar, K. G. Rajeev, V. A. Kumar, K. N. Ganesh, *Nucleic Acids Res.* **1996**, *24*, 1229; b) K. G. Rajeev, V. R. Jadhav, K. N. Ganesh, *Nucleic Acids Res.* **1997**, *25*, 4187.
[33] a) Y. Lu, B. Weers, N. C. Stellwagen, *Biopolymers* **2002**, *61*, 261; b) S. W. Kowalczyk, M. W. Tuijtel, S. P. Donkers, C. Dekker, *Nano Lett.* **2010**, *10*, 1414; c) B. Tinland, A. Pluen, J. Sturm, G. Weill, *Macromolecules* **1997**, *30*, 5763.
[34] L. C. Palmer, S. I. Stupp, *Acc. Chem. Res.* **2008**, *41*, 1674.
[35] T. Dwars, E. Paetzold, G. Oehme, *Angew. Chem.* **2005**, *117*, 7338; *Angew. Chem. Int. Ed.* **2005**, *44*, 7174.

Received: June 28, 2010
Published online: September 28, 2010

